



## Research article

# Untargeted metabolomics uncovers metabolic dysregulation and tissue sensitivity in ACE2 knockout mice

Lili Zhao<sup>1</sup>, Weili Yang<sup>1</sup>, Wenyi Ji, Qiuyue Pan, Jinkui Yang, Xi Cao<sup>\*</sup>*Beijing Diabetes Institute, Beijing Key Laboratory of Diabetes Research and Care, Department of Endocrinology, Beijing Tongren Hospital, Capital Medical University, Beijing 100730, China*

## ARTICLE INFO

## Keywords:

ACE2  
Gene knockout  
Metabolomics  
Glucolipid metabolism  
T2DM

## ABSTRACT

Angiotensin-converting enzyme 2 (ACE2) polymorphisms are associated with increased risk of type 2 diabetes mellitus (T2DM), obesity and dyslipidemia, which have been determined in various populations. Consistently, ACE2 knockout (ACE2 KO) mice display damaged energy metabolism in multiple tissues, especially the key metabolic tissues such as liver, skeletal muscle and epididymal white adipose tissue (eWAT) and show even more severe phenotype under high-fat diet (HFD) induced metabolic stress. However, the effects of ACE2 on global metabolomics profiling and the tissue sensitivity remain unclear. To understand how tissues independently and collectively respond to ACE2, we performed untargeted metabolomics in serum in ACE2 KO and control wild type (WT) mice both on normal diet (ND) and HFD, and in three key metabolic tissues (liver, skeletal muscle and eWAT) after HFD treatment. The results showed significant alterations in metabolic profiling in ACE2 KO mice. We identified 275 and 168 serum metabolites differing significantly between WT and ACE2 KO mice fed on ND and HFD, respectively. And the altered metabolites in the ACE2 KO group varied from 90 to 196 in liver, muscle and eWAT. The alterations in ND and HFD serum were most similar. Compared with WT mice, ACE2 KO mice showed an increase in N-phenylacetylglutamine (PAGln), methyl indole-3-acetate, 5-hydroxytryptophol, cholic acid, deoxycholic acid and 12(S)-HETE, while LPC (19:0) and LPE (16:1) decreased. Moreover, LPC (20:0), LPC (20:1) and PC (14:0e/6:0) were reduced in both ND and HFD serum, paralleling the decreases identified in HFD skeletal muscle. Interestingly, DL-tryptophan, indole and Gly-Phe decreased in both ND and HFD serum but were elevated in HFD liver of ACE2 KO mice. A low level of L-ergothioneine was observed among liver, muscle, and epididymal fat tissue of ACE2 KO mice. Pathway analysis demonstrated that different tissues exhibited different dysregulated metabolic pathways. In conclusion, these results revealed that ACE2 deficiency leads to an overall state of metabolic distress, which may provide a new insight into the underlying pathogenesis in metabolic disorders in both ACE2 KO mice and in patients with certain genetic variant of ACE2 gene.

<sup>\*</sup> Corresponding author. Beijing Diabetes Institute, Department of Endocrinology, Beijing Tongren Hospital, Capital Medical University, No. 1 Dongjiaominxiang, Dongcheng District, Beijing 100730, China.

E-mail address: [xicao@ccmu.edu.cn](mailto:xicao@ccmu.edu.cn) (X. Cao).

<sup>1</sup> These authors contribute equally to this paper.

<https://doi.org/10.1016/j.heliyon.2024.e27472>

Received 4 December 2023; Received in revised form 20 February 2024; Accepted 29 February 2024

Available online 8 March 2024

2405-8440/© 2024 The Authors. Published by Elsevier Ltd. This is an open access article under the CC BY-NC license (<http://creativecommons.org/licenses/by-nc/4.0/>).

## 1. Introduction

Type 2 diabetes mellitus (T2DM) is a complex disease influenced by lifestyle, environmental and genetic factors. Unlike to the first two, the genetic risk factor cannot be modified, and it tends to cause significant inter-individual differences in drug response and the occurrence of adverse drug reactions [1,2]. Therefore, understanding the changes caused by gene mutations, especially metabolic changes, is crucially important for comprehending the pathogenesis and enabling precise treatment of T2DM.

The renin angiotensin system (RAS), particularly angiotensin converting enzyme 2 (ACE2), has not only been recognized as a key component of RAS but also as the indispensable entry receptor of severe acute respiratory syndrome coronavirus (SARS CoV) and the newly outbreak respiratory syndrome coronavirus 2 (SARS CoV-2), receiving a good deal of attention in recently years. Our previous research has shown that ACE2/Ang(1–7) axis is essential in maintaining energy metabolism homeostasis in pancreatic islets, liver, epididymal white adipose tissue (eWAT), brown adipose tissue (BAT) and skeletal muscle, and that activation of the ACE2/Ang(1–7) pathway improves metabolic disorders [3–11].

The human *ACE2* gene exhibits a high degree of genetic polymorphism [12]. Nowadays, a wide variety of *ACE2* polymorphisms, including single-nucleotide polymorphisms (SNPs) are closely related to metabolic diseases. It has been reported that four *ACE2* SNPs (rs879922, rs233575, rs2158083 and rs2074192) and the haplotype (C-G-C) of the three formers were associated with a higher risk of overweight, obesity and hyperlipidemia in female Spanish adolescents [13]. In addition, a strong association was observed between the ACE2-rs4240157T > C genotypes and triglycerides, HDL-C, total cholesterol, and C-reactive protein in Tabuk [14]. Meanwhile, in China, some *ACE2* polymorphisms were also reported to be associated with gestational diabetes mellitus, T2DM, dyslipidemia, hypertriglyceridemia, and cardiovascular risk with T2DM [15–18]. Consistently, we reported that *ACE2* knockout (*ACE2* KO) mice displayed a selective decrease in first-phase insulin secretion, as well as a progressive impairment of glucose tolerance with age [19]. Furthermore, *ACE2* KO mice exhibited dysglycolipid metabolism in liver, skeletal muscle and eWAT, and impaired thermogenic function in BAT [9,20]. However, the mechanism underling the metabolic disorders in human due to the *ACE2* polymorphisms remain almost unknown, and the specific molecular mechanisms of the diabetic phenotype in mice caused by the deletion of *ACE2* are also not fully clear.

Interestingly, studies have highlighted that patients with fatal COVID-19 often exhibit metabolic perturbation, including reduced levels of plasma xylulose-5-phosphate (X-5-P) and phosphatidylcholines (PCs) [21]. Meanwhile, individual with severe COVID-19 show elevated plasma triglycerides (TGs), ceramides (Cer), and phosphatidylethanolamines (PEs), alongside a reduction in PCs and Lysophosphatidylcholines (LPCs), particularly LPC 20:1 [22]. Furthermore, the severity of COVID-19 in diabetic and hypertensive patients has been linked to long-chain polyunsaturated fatty acids (n3 and n6) [23]. More notably, research recognizes that certain *ACE2* variants increase the binding affinity to the spike protein therefore leading to more severe infections [24]. Yet, the question of whether these outcomes are driven by metabolic changes caused by *ACE2* mutations remains unanswered.

Dustin Singer et al. reported significant reduction in serum glycine (Gly) and L-tryptophan (Trp) in *ACE2* KO mice, as confirmed by UPLC measurements [25]. Similarly, Tatsuo Hashimoto et al. revealed marked decreases in the serum levels of valine (Val), threonine (Thr), tyrosine (Tyr), and Trp in *ACE2* KO mice, quantified by GC/MS [26]. Recently, Qi Chen et al. clarified that serum Trp levels were significantly reduced in *ACE2* KO mice and that this reduction could not be reversed by Trp supplementation [27]. However, to the best of our knowledge, there have been a limited number of studies conducted on metabolite changes in the serum or tissue of *ACE2* KO mice, and none have explored in impact of *ACE2* on global metabolomics profiling. Therefore, this study intends to elucidate how tissues independently and collectively respond to *ACE2* KO using untargeted metabolomics on serum from *ACE2* KO and control wild type (WT) mice, both on a normal diet (ND) and an HFD, as well as in three key metabolic tissues (liver, skeletal muscle and eWAT) after HFD treatment. The comprehensive mapping of differential metabolites due to the absence of *ACE2* may provide novel potential molecular mechanisms underlying T2DM, enhance our understanding of the elevated risk of metabolic disorder in human beings with certain *ACE2* variants and the metabolic perturbations in severe COVID-19 patients.

## 2. Materials and methods

### 2.1. Samples preparation

To evaluate the metabolomic profile changes of *Ace2* gene knockout (KO) mice under normal diet (ND) conditions, 10 male *ACE2* KO mice (*ACE2*<sup>-/-</sup>) [9] and 10 male wild-type (WT) controls were maintained on a normal diet. Approximately 200  $\mu$ L of blood was collected from the inner canthus vein of each mouse around 12 weeks ago. Then serum samples from two mice within the same group were pooled for metabolomics analysis. To evaluate the metabolomic profile changes in *ACE2* KO mice under high-fat diet (HFD) conditions, 8-week-old male *ACE2* KO mice and WT controls were subjected to an HFD for one month. Blood samples were taken from the inner canthus vein, a method that caused less stress in mice compared to other blood collection ways, then mice were anesthetized with 1% sodium pentobarbital through intraperitoneal injection at a dose of 40 mg/kg and then were sacrificed at the age of about 12-week-old, and three key metabolic tissues (liver, epididymal visceral adipose tissue, and skeletal muscle) were collected for metabolomics after cardiac perfusion with normal saline. Normal diet was purchased from Beijing Keao Xieli Feed Corporation (Beijing, China), containing 24.02% protein, 63.03% carbohydrate, and 12.95% fat. High fat diet was purchased from Research Diets, Inc. (Rodent Diet With 60 kcal% Fat, #D12492), and the main components were 26.23% protein, 25.56% carbohydrate and 34.89% fat. All mice were specific pathogen-free (SPF) experiment animal and were kept in an SPF environment with constant temperature and humidity, a 12-h/12-h dark-light cycle, dry beddings, free access to water and food. All animals were handled in accordance with the protocol approved by the Ethics Committee of Animal Research at Beijing Tongren Hospital, Capital Medical University, Beijing, China

(TRLAWEC2022-16).

## 2.2. Metabolomics analysis

Serum samples (100  $\mu$ L) was combined with 400  $\mu$ L 80% methanol (A456-4, Thermo Fisher), while tissues (100 mg) were grounded with liquid nitrogen and then mixed with 500  $\mu$ L 80% methanol. These samples were vortexed and subsequently centrifuged for 20 min at 15000 g at 4  $^{\circ}$ C after a 5-min incubation in an ice bath. A certain volume of the supernatant was then diluted with Milli-Q water (1.15333.2500, Merck) for a final concentration of 53% methanol. The mixture was centrifuged at 15000 g at 4  $^{\circ}$ C for 20 min, and the supernatant was used for LC-MS analysis.

The chromatographic instrument (Vanquish UHPLC, Thermo Fisher) fitted with the Hypersil Gold column C18 (Thermo Fisher,

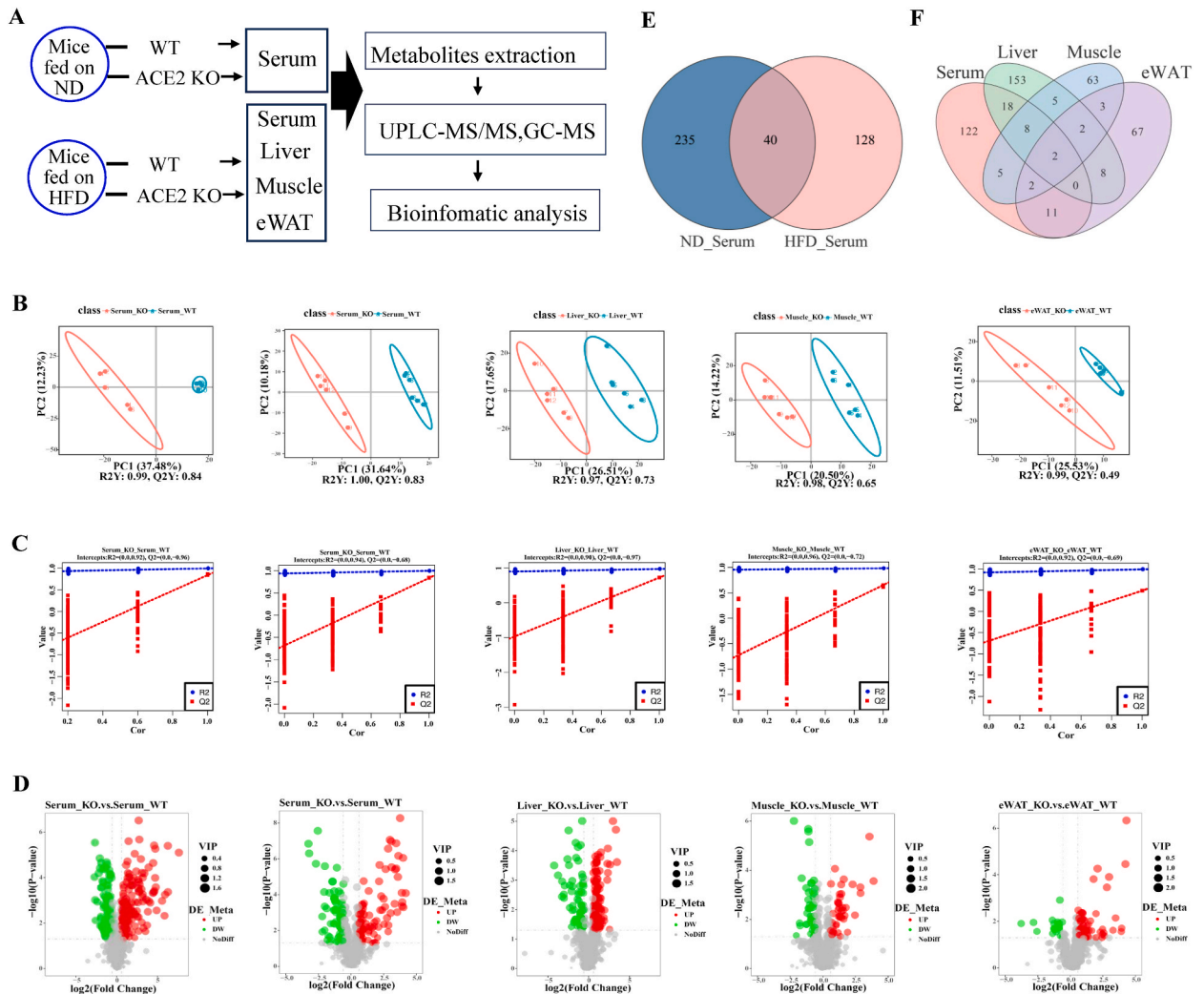


**Fig. 1.** Overview of the metabolic profiling alterations in ACE2 KO mice.

A. Schematic of the study design. Serum from ACE2 KO and WT mice fed on ND at the 12 weeks of age, and serum as well as three key metabolic tissues (liver, skeletal muscle and eWAT) from mice treated with an HFD for one month at 12 weeks of age were collected for untargeted metabolomic analysis.

B. PLS-DA plots of tissue-specific samples. The 2 groups were well separated in the PLS-DA score plot in each tissue, indicating that they had markedly different metabolic characteristics.

C. 200 permutation tests for PLS-DA models. All the red regression lines of the Q2 points intersect the vertical axis at values < 0 indicating the good reliability, predictability and no over-fitting for all the 5 PLS-DA models.

D. Volcano plots of all the detected metabolites in each tissue. Red represents upregulated, and green represents downregulated.

E. Venn diagram of changed metabolites in serum of ACE2 KO mice on different diets.

F. Venn diagram of changed metabolites in different tissues in HFD-fed ACE2 KO mice. (For interpretation of the references to color in this figure legend, the reader is referred to the Web version of this article.)

100 × 2.1 mm, 1.9 μm) was maintained at 40 °C column temperature while the flow rate was set to 0.2 ml/min. Mobile phase consisted of A (0.1% formic acid (A117-50, Thermo Fisher)) and B (methanol) in positive mode. Mobile phase consisted of A (5 mM ammonium acetate (A114-50, Thermo Fisher), pH9.0) and B (methanol) in negative mode. Elution gradient was as follows: 98% A/2% B at 0–1.5 min, 15% A/85% B at 3 min, 100% B at 10 min, 98 % A/2 % B at 10.1–12 min.

The scan range of the mass spectrometer (Q Exactive HF-X, Thermo Fisher) was set from 100 to 1500 *m/z*. The ESI source operation parameters included a spray voltage of 3.5 kV, a sheath gas flow rate of 35 psi, an auxiliary gas flow rate of 10 L/min, a capillary temperature of 320 °C, an S-lens RF level of 60, an auxiliary gas heat temperature of 350 °C, and data-dependent scans were performed.

### 2.3. Quality control

Quality control (QC) samples were prepared by mixed equal volume of extracts from each sample. The blank sample consisted of 53% methanol and was processed in the same manner as the experimental samples.

### 2.4. Statistical analysis

The data were analyzed using Compound Discoverer 3.1 software for peak annotation and metabolite identification. Metabolites were matched against the mzCloud, mzVault and Masslist databases. Annotation of metabolites utilized databases, such as Kyoto Encyclopedia of Genes and Genomes (KEGG), HMDB, Lipidmaps, and ClassyFire databases. Data procession was performed on a Linux operation (CentOS 6.6), R and Python software.

Multivariate analysis including supervised partial least square discriminant analysis (PLS-DA), was processed via metaX software, from which the variable importance in projection (VIP) value of each metabolite was acquired. Univariate analysis assessed statistical significance (P value) and fold change (FC) between two groups of each metabolite, based on the *t*-test. The criteria for identifying differential metabolites were VIP >1, P value < 0.05 and FC > 1.5 or <0.67. Volcano plots were created by R package ggplot2. Hierarchical cluster analysis was generated with the R package Pheatmap following data normalization via z-score. Radar plots were accomplished by R packages ggplot2 and fsmb. Stem plots were made with the R package ggpubr, and venn diagrams were produced by online website ([www.omicshare.com](http://www.omicshare.com)).

Bubble charts were performed using the R packages ggplot2 and ggpubr. Metabolites and their metabolic pathways were studied via KEGG database. Metabolic pathways were enriched when the ratio was satisfied by  $x/n > y/N$ . And when  $P < 0.05$ .

Correlation coefficient between differential metabolites were performed by either the Pearson or Spearman method following the Shapiro. test in the R, with a P value < 0.05 considered as statistically significant. The chord diagrams were plotted by R package circlize and the bar charts were made by Prism 9.

## 3. Results

### 3.1. Metabolic profiling alterations in ACE2 KO mice

As previously described, we reported for the first time that ACE2 KO mice displayed a selective reduction in first-phase insulin secretion and a progressive impairment in glucose tolerance as they age, alongside damage to energy metabolism in key metabolic tissues such as the liver, muscle and eWAT. Consistent with these findings, the current study demonstrated that ACE2 KO mice showed impaired glucose tolerance at the age of 12-week (Supplementary figs. S1A and B) and showed even more pronounced glucose intolerance after 4 weeks of metabolic stress induced by a HFD (from 8 to 12 weeks of age) (Supplementary figs. S1C and D). Therefore, to identify how tissues independently and collectively respond to ACE2 KO, we collected serum from ACE2 KO and WT mice fed a ND at 12 week of age, as well as serum and three key metabolic tissues (liver, skeletal muscle and eWAT) from ACE2 KO and WT mice treated with an HFD for one month at 12 weeks of age, and conducted untargeted metabolomics (Fig. 1A). We detected 845 and 726 metabolites in serum from mice on ND and HFD, respectively, and detected 647–842 metabolites in the three tissues from mice on HFD, including 543–729 metabolites annotated by KEGG, HMDB, Lipidmaps and (or) ClassyFire (Table 1, Supplementary tables S1 and S2). Furthermore, 115 annotated metabolites were detected in all tissues and serum (Table 1, Supplementary table S3).

Supervised partial least square discriminant analysis (PLS-DA) revealed a clear separation between the ACE2 KO and WT groups (ND-serum: R2Y = 0.99, Q2Y = 0.84; HFD-serum: R2Y = 1.00, Q2Y = 0.83; HFD-liver: R2Y = 0.97, Q2Y = 0.73; HFD-muscle: R2Y = 0.98, Q2Y = 0.65; HFD-eWAT: R2Y = 0.99, Q2Y = 0.49). The values close to 1.0 for all the 5 models indicated their stability and

**Table 1**  
Detected metabolites including annotated and unannotated metabolites.

Tissue	Total	Annotated by KEGG, HMDB, Lipidmaps and (or) ClassyFire
ND Serum	845	729
HFD Serum	726	622
HFD Liver	842	648
HFD Muscle	806	669
HFD eWAT	647	543
Universal		115

predictive reliability (Fig. 1B). Permutation tests with 200 iterations were performed to investigate whether the PLS-DA models underwent data over-fitting. All the red regression line of the Q2 points intersect the vertical axis at values  $< 0$  indicating the good reliability, predictability and no over-fitting for all the 5 PLS-DA models (Fig. 1C). These results imply significant differences in their metabolites between WT and ACE2 KO mice. Then volcano plot analysis was applied to screen out potential differential metabolites accounting for the differentiation. Metabolites with VIP values  $> 1$ ,  $p < 0.05$  and  $FC > 1.5$  or  $< 0.67$  were regarded as significantly different metabolites (Fig. 1D). Based upon our criteria, ACE2 KO mice fed on ND altered 275 serum metabolites, whereas 168 serum metabolites were impacted by ACE2 KO in mice fed on HFD. This included 40 metabolites common to both diets, and 235 (ND) and 128 (HFD) metabolites specific to each (Fig. 1E– Supplementary table S4). The altered tissue metabolites in the ACE2 KO mice fed on HFD ranged from 90 to 196, and some of these differential metabolites were present in at least three different tissues simultaneously. There included 2 metabolites (phenylacetyl glycine (PAGly), corticosterone) common to serum and 3 tissues, 2 metabolites (L-ergothioneine, cytidine) common to 3 tissues, 2 metabolites (3-Indoxyl sulfate, LPC 20:0) common to serum, muscle and eWAT, 8 metabolites (isoquinoline, thymidine, thymine, DL-tryptophan, 6-methylquinoline, tetrahydroaldosterone, lysopc 16:2 (2 N Isomer),  $\beta$ -Cortolone) common to serum, muscle and liver (Fig. 1F– Supplementary table S5). To further evaluate the differences in metabolism between the ACE2 KO and WT groups in detail, we created heatmap images to visualize the differential metabolites. Consistent with the results of the PLS-DA, most samples clearly showed consistent inter-group differences and minimal intra-group differences (Supplementary figs. S2A–D). These results revealed that serum and each tissue displayed unique metabolic responses to ACE2 deficiency. Thus, loss of ACE2 had a diet and tissue-specific impact on metabolites.

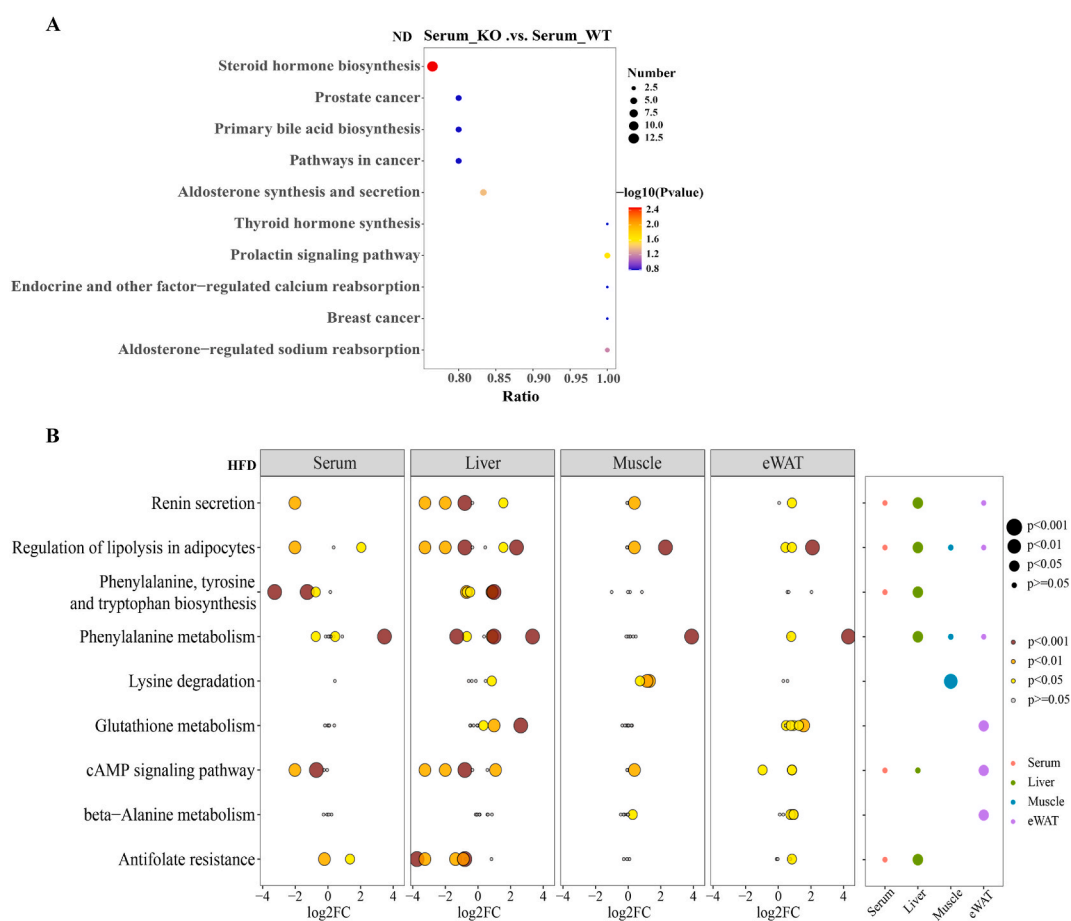


**Fig. 2.** Summary of pathway analysis of changed metabolites affected by ACE2 deletion.

A. KEGG enrichment analysis of changed serum metabolites in ND-fed ACE2 KO mice. The ratio refers to the proportion of differential metabolites to the total metabolites in the pathway. The color and size of each circle are based on pathway  $-\log_{10}(p\text{-value})$  and the number of differential metabolites, respectively.

B. Pathways enriched significantly in at least one tissue in HFD-fed ACE2 KO mice. Tissue-specific dotplots show regulation of metabolites mapped to specific pathways.  $\log_2 FC$  (fold change) refers to the regulation of metabolites induced by ACE2 deletion. The size and color of each dot indicate significance of regulated (P-value) metabolites. Gray dots refer to metabolites mapped to the pathway but not significantly regulated. The significance of pathway enrichment is displayed on the right-side dotplot. The color of dots refers to tissue, and size refers to enrichment significance (P-value). (For interpretation of the references to color in this figure legend, the reader is referred to the Web version of this article.)

### 3.2. Metabolic pathways affected by ACE2 deletion

To identify which metabolic pathways were directly impacted by ACE2 deletion, we performed KEGG enrichment analysis on the significantly altered metabolites. The differential serum metabolites in ACE2 KO mice on a ND were linked to 44 KEGG pathways (Supplementary table S6) and the top 10 pathways, ranked by the P-value, were shown in the bubble chart (Fig. 2A), with 3 pathways

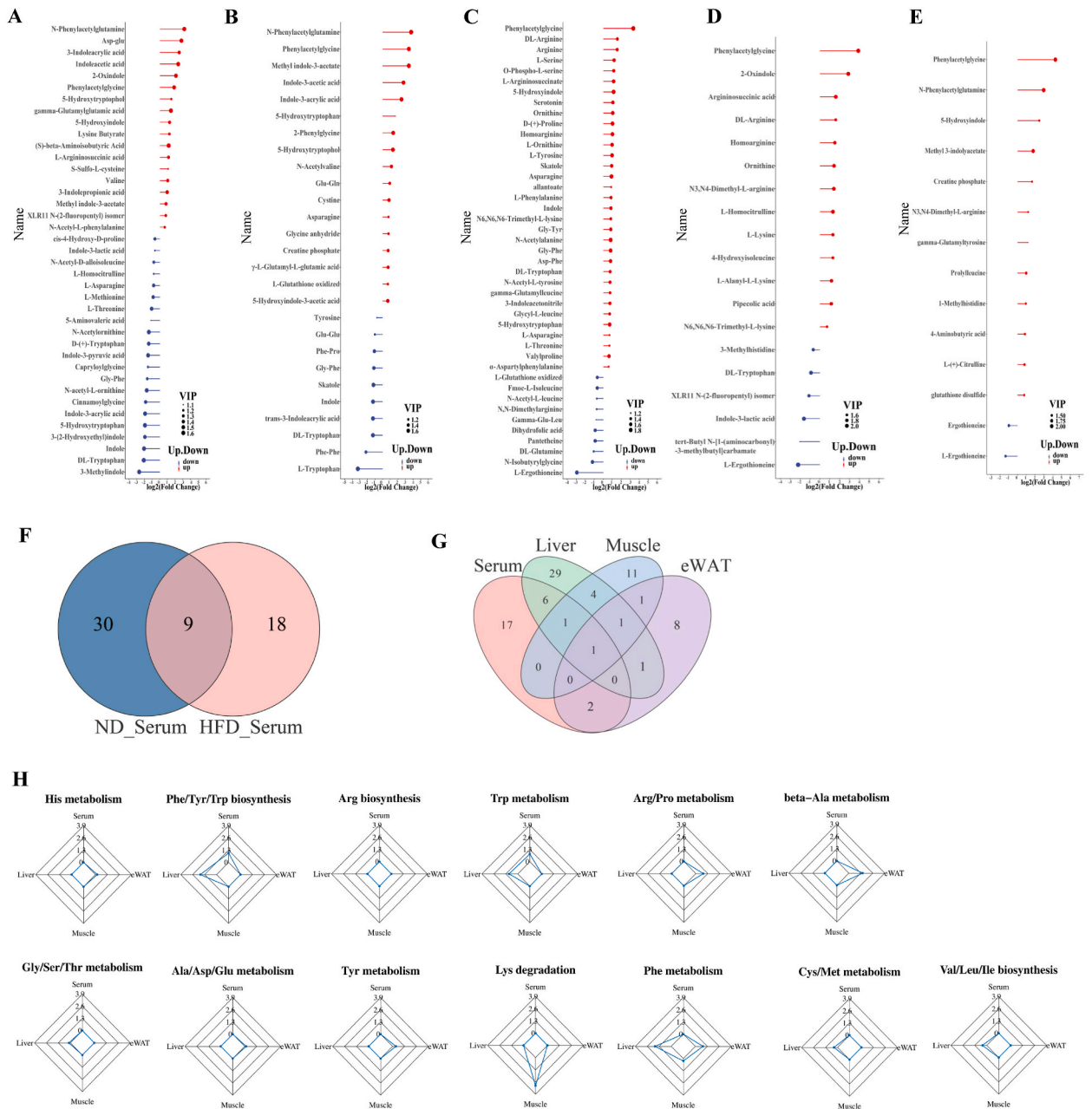


**Fig. 3.** Summary of amino acid metabolism affected by ACE2 deletion.

A-E. Stem plot analysis of differential AAs and derivatives in serum (A) of ND-fed ACE2 KO mice, and in serum (B), liver (C), muscle (D) and eWAT (E) of HFD-fed ACE2 KO mice. The stem and size of each circle are based on Log2 (fold change) and VIP value of differential metabolites, respectively. Red color represents upregulated, while blue color represents downregulated.

F. Venn diagram of changed AAs and derivatives in serum of ACE2 KO mice under different diet.

G. Venn diagram of changed AAs and derivatives in different tissues in HFD-fed ACE2 KO mice.

H. Radar plots representing tissue-specific enrichment of regulated metabolites related to each amino acid class affected by ACE2 deletion. The first, second, third, and fourth lines from the center indicate  $-\log_{10} p\text{-value} = 0, 1.3, 2.6,$  and  $3.9,$  respectively. (For interpretation of the references to color in this figure legend, the reader is referred to the Web version of this article.)

(Steroid hormone biosynthesis, Aldosterone synthesis and secretion, and Prolactin signaling pathway) showing significant enrichment ( $P < 0.05$ ). Meanwhile, the differential metabolites in serum, liver, muscle and eWAT in ACE2 KO mice fed on a HFD were enriched in 54, 73, 17, and 54 KEGG pathways, respectively (Supplementary table S7). Of these, 9 pathways enriched significantly in at least one tissue, including 5 (phenylalanine metabolism, phenylalanine, tyrosine and tryptophan biosynthesis, antifolate resistance, regulation of lipolysis in adipocytes, and renin secretion) in the liver; one (lysine degradation) in the muscle, and 3 (cAMP signaling pathway, beta-Alanine metabolism, and glutathione metabolism) in the eWAT (Fig. 2B). These findings revealed that loss of ACE2 led to a robust enrichment of pathways, especially those involved in amino acids (AAs) metabolism. Consistent with the variations in altered metabolites described previously, each tissue displayed significantly different enriched pathways.

### 3.3. Amino acids metabolism affected by ACE2 deletion

Since amino acids metabolism exhibited the most significant differences in the ACE2 KO group, as evidenced by the KEGG enrichment pathway analysis, we explored the diet and tissue dependencies of ACE2 deletion on amino acids metabolism. This analysis include data on amino acids, peptides, and analogues, as well as indoles and derivatives. Heatmaps displayed that a majority of the samples clearly showed consistent inter-group differences and minimal intra-group differences for most of the differential amino acids and derivatives in the serum of mice fed on a ND as well as in the serum, liver, muscle and eWAT of mice fed on a HFD (Supplementary figs. S3A–E). Subsequently, stem plot analysis was performed to visualize the differences with FC and VIP value (Fig. 3A–E). As presented in stem plots, there were 12 more different amino acids and derivatives in serum of ACE2 mice fed on ND than those fed on HFD, but serum N-phenylacetylglutamine, PAGly, 5-Hydroxytryptophol, and methyl indole-3-acetate were increased while Gly-Phe, indole and DL-Trp were decreased in ACE2 KO mice, regardless of being fed on ND and HFD. The reduced DL-Trp level in ACE2 KO mice was consistent with results reported in the literature [25,26]. Among the 9 common differential serum AA and derivatives between ND and HFD, although these 7 showed the same trend, two exhibited the opposite trend: indole-3-acrylic acid and 5-Hydroxytryptophan were significantly reduced in ACE2 KO mice fed on ND but remarkably raised in those fed on HFD (Fig. 3F–Supplementary table S8). These results suggest that the impact of ACE2 knockout on amino acids metabolism is obviously diet-dependent.

In HFD-fed ACE2 KO mice, the liver showed the most significant alterations in AAs and derivatives, while eWAT showed the least. The liver and serum responses to ACE2 deletion in terms of AA metabolism were significantly different, and among the 6 amino acids and derivatives common to both liver and serum, most changes were opposite: Gly-Phe, skatole, and indole decreased in serum but

**Table 2**  
Differential steroid hormones metabolites in WT and ACE2 KO group.

Tissue	Metabolites	FC	log2FC	Pvalue	VIP	Up/Down	
ND Serum	Aldosterone	77.26	6.27	0.00043	1.58	up	
	Cortisone	27.53	4.78	0.00027	1.59	up	
	Cortisol	24.42	4.61	0.00039	1.58	up	
	Tetrahydroaldosterone	22.05	4.46	2.30E-05	1.62	up	
	Hydrocortisone acetate	14.08	3.82	0.00318	1.49	up	
	5alpha-Pregnane-3,20-dione	7.80	2.96	1.54E-05	1.58	up	
	Guggulsterone	6.45	2.69	3.09E-07	1.64	up	
	17 alpha-Ethinyl estradiol	3.73	1.90	0.00022	1.51	up	
	Estrone	3.22	1.69	0.00209	1.40	up	
	7alpha-Hydroxytestosterone	2.88	1.53	7.05E-05	1.55	up	
	Corticosterone	2.57	1.36	0.00404	1.37	up	
	Progesterone	2.48	1.31	0.00800	1.29	up	
	Estradiol	2.40	1.26	0.00164	1.51	up	
	21-Deoxycortisol	1.93	0.95	0.00708	1.30	up	
	Boldione	1.87	0.90	0.02435	1.17	up	
	Tetrahydrocortisone	1.73	0.79	0.00050	1.48	up	
	5 beta-Androstane-3,17-dione	0.57	-0.81	0.02023	1.31	down	
	HFD Serum	Estrone	7.20	2.85	2.72E-07	1.78	up
		Corticosterone	4.12	2.04	0.02507	1.16	up
		Tetrahydroaldosterone	3.39	1.76	0.00597	1.39	up
Boldione		0.61	-0.70	0.03271	1.11	down	
Pregnenolone		0.42	-1.26	0.00070	1.54	down	
Corticosterone		5.14	2.36	0.00056	1.75	up	
HFD Liver	Methyltestosterone	2.72	1.44	0.00144	1.65	up	
	Tetrahydroaldosterone	1.90	0.93	0.02562	1.34	up	
	11-Ketoetiocholanolone	1.79	0.84	0.02801	1.29	up	
	Estrone	1.72	0.78	0.00217	1.64	up	
	Cortisol	1.59	0.67	0.03185	1.30	up	
	Estriol	0.56	-0.85	0.04762	1.33	down	
	Aldosterone	7.42	2.89	0.00086	1.92	up	
HFD Muscle	Corticosterone	4.87	2.28	0.00038	2.00	up	
	Tetrahydroaldosterone	1.72	0.79	0.00580	1.78	up	
	Boldione	11.11	3.47	0.00718	1.72	up	
HFD eWAT	Corticosterone	4.27	2.10	5.45E-05	2.18	up	

increased in the liver. Meanwhile, L-glutathione oxidized increased in serum while decreasing in the liver. Among differential metabolites present in at least three different tissues simultaneously, we found 1) L-ergothioneine was downregulated in liver, muscle and eWAT; 2) DL-Trp decreased in serum and muscle while increased in liver; and 3) only PAGly was uniformly elevated across serum, liver, muscle, and eWAT in HFD-fed ACE2 KO mice. Other amino acids and derivatives that differed only between two tissues showed similar trends: creatine phosphate and N-phenylacetylglutamine increased in both serum and eWAT. Ornithine, DL-arginine, homo-arginine, and N6,N6,N6-Trimethyl-L-lysine were upregulated in both liver and muscle. 5-Hydroxyindole increased in both liver and eWAT. N3,N4-Dimethyl-L-arginine elevated in both muscle and eWAT (Fig. 3G–Supplementary table S9). The differential AAs and derivatives in serum, liver, muscle and eWAT in HFD-fed ACE2 KO mice were enriched in 3, 7, 2, and 6 KEGG pathways, respectively (Supplementary table S10). Of these, 4 pathways were significantly enriched: phenylalanine metabolism ( $p = 0.017$ ) and phenylalanine, tyrosine, and tryptophan biosynthesis ( $p = 0.017$ ) in the liver; lysine degradation ( $p = 0.001$ ) in muscle; and beta-Alanine metabolism ( $p = 0.031$ ) in eWAT (Fig. 3H–Supplementary table S10). These findings highlight the significant differences in the response of various tissues to ACE2 deletion, yet also point to a certain degree of correlation.

### 3.4. Steroid hormone metabolism affected by ACE2 deletion

According to the KEGG enrichment analysis, the predominant significantly enriched metabolic pathways associated with ACE2 deletion in ND-fed mice were related to steroid hormone metabolism, including steroid hormone biosynthesis ( $p = 0.003$ ) and aldosterone synthesis and secretion ( $p = 0.04$ ) (Supplementary table S6). In HFD-fed ACE2 mice, the altered metabolites were also enriched in several metabolism related to steroid hormone metabolism, but thesis did not reach statistical significance, This included 4 pathways (cortisol synthesis and secretion, aldosterone synthesis and secretion, ovarian steroidogenesis, and steroid hormone biosynthesis) in serum, 4 pathways (aldosterone synthesis and secretion, steroid hormone biosynthesis, cortisol synthesis and secretion and aldosterone-regulated sodium reabsorption) in liver, and 3 pathways (aldosterone-regulated sodium reabsorption, steroid hormone biosynthesis and aldosterone synthesis and secretion) in muscle. However, no steroid hormone metabolism related pathways were enriched in eWAT (Supplementary table S7).

Corresponding to the results of the KEGG enrichment analysis, ND-fed ACE2 KO mice exhibited the highest levels of serum steroids and steroid derivatives with significant differences, among which, except for 5 beta-Androstane-3, 17-Dione, which was significantly down-regulated, the rest were significantly up-regulated. In HFD-fed ACE2 KO mice, the liver displayed the most, while eWAT showed the least markedly changed steroids and steroid derivatives. Among these changes, boldione showed the most significant alteration in both serum and eWAT. Additionally, estrone levels were increased in both serum and liver, while tetrahydroaldosterone levels were elevated in serum, liver, and muscle. Corticosterone levels consistently increased in serum in both ND- and HFD-fed ACE2 KO mice and in 3 tissues in HFD-fed ACE2 KO mice (Table 2, Supplementary table S11). Elevated serum levels of corticosterone, cortisol, and cortisone has been persistently observed in T2DM patients and animal models, with corticosterone also shown to disrupt glucose metabolism [28]. Estrone plays a crucial role in the regulation of glucose metabolism, and its levels are positively associated with glucose levels and gestational diabetes in mid-late pregnancy [29,30]. These results suggest that the disordered steroid hormone metabolism may contribute to the disorganized energy metabolism observed in ACE2 KO mice.

**Table 3**  
Differential carbohydrates and carbohydrate conjugates in WT and ACE2 KO group.

Tissue	Metabolites	FC	log2FC	Pvalue	VIP	Up.Down
ND Serum	D(-)-Fructose	0.66	-0.60	0.01379	1.23	down
	D-Glucose 6-phosphate	0.59	-0.77	0.00542	1.32	down
	N-Acetylneuraminic acid	0.36	-1.47	0.01509	1.24	down
	D-Xylulose 5-phosphate	0.19	-2.39	0.00117	1.44	down
HFD Serum	Indoxyl-β-D-glucuronide	10.16	3.34	0.00032	1.68	up
	Gluconic acid	1.55	0.64	0.00401	1.40	up
	D(-)-Fructose	0.66	-0.61	0.02474	1.21	down
HFD Liver	Maltotriose	0.63	-0.67	0.00136	1.64	down
	D-Fructose 1-phosphate	0.61	-0.71	0.00122	1.65	down
	D-Ribose-1-phosphate	0.58	-0.80	0.00001	1.91	down
	5'-Adenylic acid	0.57	-0.81	0.00063	1.70	down
	Gluconolactone	0.55	-0.86	0.01930	1.36	down
	Glucose-1-phosphate	0.51	-0.96	0.01883	1.35	down
	α-Cyclodextrin	0.48	-1.06	0.01969	1.34	down
	β-D-Glucopyranuronic acid	0.44	-1.18	0.00257	1.65	down
	D-Glucose 6-phosphate	0.42	-1.26	0.00022	1.77	down
	D-Mannose 6-phosphate	0.26	-1.96	0.00164	1.68	down
	s7p	2.31	1.21	0.00776	1.67	up
HFD Muscle	Sedoheptulose 1,7-bisphosphate	0.64	-0.64	0.00057	1.94	down
	D-Threose	9.70	3.28	0.02393	1.58	up
HFD eWAT	Cyclic ADP-ribose	2.71	1.44	0.02449	1.42	up
	N-Acetyl-D-galactosamine 4-sulfate	1.53	0.62	0.00332	1.75	up
	D-Ribose	0.38	-1.38	0.00882	1.56	down

**Table 4**  
Differential glycerophospholipids in WT and ACE2 KO group.

Tissue	Metabolites	FC	log2FC	Pvalue	VIP	Up,Down	
ND Serum	Phosphatidylinositol-1,2-dipalmitoyl	57.88	5.85	0.00476	1.48	up	
	LPA 17:0	2.77	1.47	0.00875	1.38	up	
	LPE 17:0	2.48	1.31	0.00002	1.58	up	
	PC (20:1/20:2)	2.33	1.22	0.00016	1.56	up	
	1-Palmitoyl-Sn-Glycero-3-Phosphocholine	2.26	1.18	0.01879	1.33	up	
	LPC 15:0	2.20	1.14	0.00087	1.45	up	
	PC (7:0/8:0)	1.95	0.96	0.01554	1.35	up	
	LPC 17:0	1.94	0.95	0.04088	1.12	up	
	PC (14:0e/3:0)	1.75	0.81	0.00127	1.43	up	
	PC (22:4e/16:0)	1.64	0.72	0.00679	1.39	up	
	PC (9:0/9:0)	1.50	0.59	0.03943	1.14	up	
	LPI 16:0	0.66	-0.60	0.01097	1.26	down	
	LPE 18:3	0.61	-0.71	0.00182	1.45	down	
	PC (20:3e/2:0)	0.61	-0.72	0.01878	1.21	down	
	LPC 18:4	0.60	-0.74	0.00007	1.54	down	
	PC (16:2e/6:0)	0.57	-0.81	0.01473	1.32	down	
	LPC 20:5	0.55	-0.88	0.00594	1.38	down	
	LPE 20:5	0.54	-0.89	0.00644	1.43	down	
	LPE 16:1	0.53	-0.93	0.00095	1.47	down	
	LPC 17:2	0.52	-0.94	0.00005	1.56	down	
	LPG 16:1	0.52	-0.95	0.00225	1.39	down	
	PA (18:1/18:1)	0.51	-0.98	0.01493	1.24	down	
	LPA 20:5	0.49	-1.02	0.00546	1.33	down	
	PC (2:0/18:3)	0.49	-1.03	0.01975	1.21	down	
	LPE 20:0	0.49	-1.03	0.01482	1.22	down	
	LPC 19:0	0.48	-1.04	0.01425	1.28	down	
	PE (18:2/18:2)	0.48	-1.05	0.00102	1.45	down	
	PC (18:4e/2:0)	0.46	-1.12	0.00116	1.52	down	
	PG (16:0/18:1)	0.45	-1.15	0.00422	1.34	down	
	PC (18:5e/2:0)	0.42	-1.25	0.00022	1.52	down	
	PC (14:0e/5:0)	0.42	-1.26	0.00877	1.40	down	
	LPE 20:1	0.42	-1.27	0.00087	1.45	down	
	PC (17:0/18:1)	0.40	-1.33	0.04252	1.08	down	
	LPC 20:1	0.38	-1.39	0.00004	1.58	down	
	LPC 22:1	0.36	-1.48	0.00678	1.30	down	
	PC (18:0/19:1)	0.35	-1.51	0.03519	1.19	down	
	PC (18:1e/2:0)	0.32	-1.63	0.00152	1.52	down	
	PC (16:1e/5:0)	0.28	-1.82	0.01443	1.24	down	
	PC (14:0e/6:0)	0.24	-2.06	0.01346	1.29	down	
	LPC 20:0	0.15	-2.74	0.00010	1.55	down	
	HFD Serum	LPG 18:1	2.60	1.38	0.01040	1.27	up
		LPS 18:0	2.27	1.19	0.00644	1.40	up
LPI 18:0		1.68	0.75	0.01255	1.29	up	
Lysops 22:6		1.67	0.74	0.00354	1.39	up	
LPC 20:1		0.67	-0.59	0.00916	1.33	down	
LPI 18:2		0.66	-0.60	0.04574	1.06	down	
Lysopa 16:0		0.65	-0.62	0.03802	1.11	down	
LPE 16:1		0.64	-0.65	0.00184	1.47	down	
LPC 19:0		0.58	-0.78	0.00764	1.39	down	
PC (14:0e/6:0)		0.45	-1.16	0.00326	1.52	down	
PC (6:0/16:2)		0.44	-1.17	0.00067	1.58	down	
LPC 20:0		0.42	-1.25	0.00437	1.42	down	
LPI 20:3		0.32	-1.65	0.00008	1.61	down	
HFD Liver		Lysopc 14:0	2.47	1.31	0.04509	1.28	up
		PC (18:0/18:1)	2.23	1.16	0.02446	1.37	up
		LPS 22:4	0.66	-0.60	0.01023	1.45	down
		LPC 18:4	0.61	-0.71	0.03252	1.27	down
		PS (19:2/19:2)	0.53	-0.91	0.04517	1.22	down
	LPI 18:2	0.53	-0.92	0.01880	1.43	down	
	PC (20:3/20:4)	0.39	-1.37	0.03649	1.27	down	
	Lysopg 18:1	0.30	-1.75	0.01017	1.49	down	
HFD Muscle	PC (18:1/18:1)	0.28	-1.86	0.02750	1.32	down	
	PC (22:4e/18:4)	3.22	1.69	0.00703	1.68	up	
	LPG 18:2	2.56	1.35	0.04833	1.43	up	
	PE (16:0/20:4)	1.51	0.60	0.02807	1.43	up	
	LPC 20:1	0.66	-0.60	0.01602	1.55	down	
	LPE 20:0	0.64	-0.64	0.02729	1.46	down	
LPE 22:6	0.63	-0.66	0.00733	1.69	down		

(continued on next page)

**Table 4** (continued)

Tissue	Metabolites	FC	log2FC	Pvalue	VIP	Up.Down
HFD eWAT	LPC 17:1	0.63	-0.66	0.00090	1.96	down
	LPE 22:5	0.59	-0.77	0.00327	1.76	down
	PC (18:5e/4:0)	0.52	-0.95	0.00753	1.70	down
	LPC 20:0	0.51	-0.96	0.01125	1.65	down
	LPC 22:6	0.50	-1.01	0.00256	1.80	down
	PC (14:0e/6:0)	0.48	-1.06	0.00352	1.79	down
	LPI 18:0	0.29	-1.78	0.01399	1.71	down
	PC (20:4e/20:5)	4.89	2.29	0.02841	1.42	up
	Lysope 18:1	3.92	1.97	0.00467	1.61	up
	Lysopc 20:4	2.00	1.00	0.01469	1.50	up
	PC (14:0e/3:0)	1.88	0.91	0.03718	1.38	up
	LPC 18:1	1.82	0.87	0.00426	1.72	up
	1-Palmitoyl-Sn-Glycero-3-Phosphocholine	1.79	0.84	0.02809	1.41	up
	PC (5:0/13:1)	1.75	0.81	0.04717	1.28	up
	Lysopc 18:1	1.63	0.71	0.02671	1.43	up
	PE (16:1e/22:6)	0.65	-0.61	0.04472	1.28	down
	PE (16:1e/16:1)	0.56	-0.84	0.01742	1.45	down
	LPC 20:0	0.55	-0.87	0.01873	1.68	down

### 3.5. Carbohydrates metabolism affected by ACE2 deletion

Carbohydrate pathways were significantly associated with T2DM, and impaired carbohydrate metabolism inducing hyperglycemia is the major metabolic disorder of non-insulin-dependent diabetes mellitus [31,32]. In this study, we found that serum D-(–)-fructose was markedly reduced in both ND and HFD fed ACE2 KO mice, which is typically altered in individuals with T1DM and T2DM [33]. Besides, serum D-glucose 6-phosphate, N-acetylneuraminic acid, and D-xylulose 5-phosphate were downregulated in ND-fed ACE2 KO mice, while indoxyl-β-D-glucuronide and gluconic acid were upregulated in those fed on HFD. In HFD-fed ACE2 KO mice, carbohydrates and carbohydrate conjugates were also changed in liver, muscle and eWAT, with the liver showing the most and the muscle showing the least markedly changed carbohydrates and carbohydrate conjugates, suggesting the vital role of liver in the carbohydrates metabolism (Table 3, Supplementary table S12).

### 3.6. Lipid metabolism affected by ACE2 deletion

It is reported that glycerophospholipids accounted for the largest proportion of the detected lipids categories in the T2DM-associated hyperlipidemia patients and healthy controls, and the glycerophospholipid metabolism pathway was also the most relevant pathway with T2DM-associated hyperlipidemia for these lipid metabolisms [34]. Therefore, to gain insight into the effects of ACE2 deletion on lipid metabolism, we focused on differential lipids in ACE2 KO mice, especially glycerophospholipids. A large amount of significantly differential glycerophospholipids were selected using the criteria of VIP values > 1, p values < 0.05 and FC > 1.5 or < 0.67. In ND-fed ACE2 KO mice, phosphatidylinositol-1, 2-Dipalmitoyl, LPA 17:0, LPE 17:0 and other 8 glycerophospholipids

**Table 5**

Differential bile acids, alcohols and derivatives in WT and ACE2 KO group.

Tissue	Metabolites	FC	log2FC	Pvalue	VIP	Up.Down	
ND Serum	7-Ketolithocholic acid	47.02	5.56	0.00107	1.55	up	
	Deoxycholic acid	26.45	4.73	0.00001	1.60	up	
	Dehydrocholic acid	23.10	4.53	0.00045	1.59	up	
	3-dehydrocholic acid	21.51	4.43	0.00048	1.57	up	
	Lithocholic Acid	12.35	3.63	0.00092	1.56	up	
	Cholic acid	9.06	3.18	0.00054	1.51	up	
	Glycocholic acid	2.87	1.52	0.04088	1.17	up	
	Hyodeoxycholic acid	2.40	1.26	0.00112	1.47	up	
	Isolithocholic acid	0.47	-1.08	0.02025	1.19	down	
	Taurocholic acid	0.42	-1.24	0.01860	1.24	down	
	Taurohyocholic acid sodium salt	0.36	-1.47	0.01093	1.31	down	
	HFD Serum	Chenodeoxycholic Acid	7.19	2.85	0.01161	1.37	up
		Deoxycholic Acid	6.30	2.65	0.00000	1.71	up
Cholic acid		6.12	2.61	0.00048	1.57	up	
3-Oxo-7alpha,12alpha-hydroxy-5 beta-cholanoic acid		5.75	2.52	0.00455	1.42	up	
Taurocholic acid		5.24	2.39	0.00073	1.53	up	
Taurodeoxycholic Acid		3.36	1.75	0.01612	1.31	up	
7-Ketolithocholic acid		3.08	1.62	0.00714	1.36	up	
HFD Liver	Glycocholic acid	2.23	1.16	0.03999	1.32	up	
	3-Oxo-7alpha,12alpha-hydroxy-5 beta-cholanoic acid	2.11	1.08	0.02129	1.35	up	
	Taurochenodeoxycholic acid	1.83	0.88	0.01472	1.46	up	

were significantly elevated, while LPI 16:0, LPE 18:3, PC (20:3e/2:0), and other 26 glycerophospholipids were significantly decreased in the serum. In HFD-fed ACE2 KO mice, LPG 18:1, LPS 18:0, LPI 18:0, and Lysops 22:6 were significantly increased, while LPC 20:1, LPI 18:2, Lysopa 16:0 and other 6 glycerophospholipids were markedly reduced in serum. Lysopc 14:0, and PC (18:0/18:1) were significantly upregulated, while LPS 22:4, LPC 18:4, PS (19:2/19:2) and other 4 glycerophospholipids were markedly downregulated in the liver. PC (22:4e/18:4), LPG 18:2, and PE (16:0/20:4) were significantly elevated, while LPC 20:1, LPE 20:0, LPE 22:6 and other 7 glycerophospholipids were markedly reduced in muscle. PC (20:4e/20:5), Lysope 18:1, Lysopc 20:4 and other 5 glycerophospholipids were significantly increased, while PE (16:1e/22:6), PE (16:1e/16:1) and LPC 20:0 were markedly decreased in eWAT (Table 4, Supplementary table S13). These results indicated the diet and tissue dependences of significantly response to ACE2 deletion in lipid metabolism.

### 3.7. Bile acids metabolism affected by ACE2 deletion

Bile acids are crucial regulatory molecules in metabolic diseases and are becoming potential targets, with some being used for the prevention or treatment of diseases such as primary biliary cirrhosis [35]. We then focused on significantly differential metabolites in bile acids, alcohols and derivatives subclass. In ND-fed ACE2 KO mice, 7-Ketolithocholic acid, deoxycholic acid, dehydrocholic acid, and other 5 bile acids, alcohols and derivatives were significantly increased, while isolithocholic acid, taurocholic acid, and taurohyocholic acid sodium salt were notably decreased in serum. In HFD-fed ACE2 KO mice, bile acids, alcohols and derivatives in muscle and eWAT did not alter significantly, but there were 7 markedly upregulated ones in serum and 3 significantly elevated ones in liver (Table 5, Supplementary table S14).

### 3.8. Eicosanoid metabolism affected by ACE2 deletion

Eicosanoids, which are widely involved in T1DM and T2DM, are derived from the arachidonic acid through three pathways: the cyclooxygenase (COX), lipoxygenase (LOX), and cytochrome P450 (CYP) pathways, including prostaglandins (PGs), thromboxanes (TXs), and hydroxyeicosatetraenoic acids (HETEs), leukotrienes (LTs), and epoxyeicosatrienoic acids (EETs) [36,37]. In ND-fed ACE2 KO mice, 8-iso-15-keto prostaglandin E2 (PGE2), 11-Deoxy PGF1 $\alpha$ , 16,16-Dimethyl PGA1, and other 9 eicosanoids were remarkably increased, while PGK2 and 11beta-PGF2 $\alpha$  were significantly decreased in serum. In HFD-fed ACE2 KO mice, there were no significantly altered eicosanoids in muscle. 12(S)-HETE, thromboxane B3 (TXB3), and 15-Deoxy- $\Delta$ 12,14-PGA1 were markedly elevated, while PGG2 and PGE2 were significantly reduced in serum. PGE2 and thromboxane B1 (TXB1) were substantially decreased in liver. TXB3 and 6-Keto PGF1 $\alpha$  were significantly upregulated, while PGB2 was markedly downregulated in eWAT (Table 6, Supplementary table S15). Among these significantly altered eicosanoids, 12(S)-HETE, reported to be increased in the serum of T2DM patients and to promotes islet  $\beta$ -cell dysfunction and  $\beta$ -cell destruction [36], was elevated in serum in both ND and HFD fed ACE2 KO mice. These findings may give new insight into the biology underlying impaired pancreatic beta cell function in ACE2 KO mice.

**Table 6**  
Differential eicosanoids in WT and ACE2 KO group.

Tissue	Metabolites	FC	log2FC	Pvalue	VIP	Up.Down
ND Serum	8-iso-15-keto Prostaglandin E2	60.50	5.92	0.00057	1.56	up
	11-Deoxy prostaglandin F1 $\alpha$	15.35	3.94	0.00108	1.55	up
	16,16-Dimethyl prostaglandin A1	13.21	3.72	0.01247	1.38	up
	2,3-Dinor-TXB2	8.36	3.06	0.00922	1.36	up
	19(R)-hydroxy Prostaglandin A2	6.46	2.69	0.00016	1.57	up
	19(R)-Hydroxy-prostaglandin E2	3.24	1.70	0.00022	1.52	up
	20-Carboxy-Leukotriene B4	2.77	1.47	0.00033	1.55	up
	16,16-Dimethyl prostaglandin A2	2.14	1.10	0.00899	1.38	up
	12(S)-HETE	1.82	0.87	0.02254	1.17	up
	8-Iso prostaglandin A2	1.68	0.75	0.00253	1.39	up
	13,14-dihydro-15-keto Prostaglandin A2	1.65	0.73	0.00208	1.41	up
	5-trans prostaglandin F2 $\beta$	1.65	0.72	0.00236	1.41	up
	Prostaglandin K2	0.55	-0.85	0.01095	1.26	down
	11beta-Prostaglandin F2alpha	0.49	-1.03	0.02032	1.23	down
	HFD Serum	12(S)-HETE	1.72	0.79	0.04898	1.04
Thromboxane B3		1.61	0.69	0.04878	1.06	up
15-Deoxy- $\Delta$ 12,14-prostaglandin A1		1.61	0.68	0.01479	1.26	up
Prostaglandin G2		0.28	-1.82	0.03364	1.17	down
Prostaglandin E2		0.25	-2.02	0.00955	1.34	down
HFD Liver	Prostaglandin E2	0.25	-2.01	0.00105	1.75	down
	Thromboxane B1	0.18	-2.46	0.00002	1.94	down
HFD eWAT	Thromboxane B3	2.36	1.24	0.02507	1.48	up
	6-Ketoprostaglandin F1 $\alpha$	1.77	0.83	0.04011	1.35	up
	Prostaglandin B2	0.42	-1.26	0.02025	1.68	down

### 3.9. Correlations in differential metabolites within tissues affected by ACE2 deletion

Since the six metabolite classes (amino acids and indoles metabolites; carbohydrates and carbohydrates conjugates; glycerophospholipids; bile acids, alcohols, and derivatives; eicosanoids; steroid hormones metabolites) described above showed significant alterations due to ACE2 deletion and all these alterations show a certain degree of dietary and tissue dependence, we further analyzed the correlations among the differential metabolites within these six metabolite classes in the serum, liver, muscle and eWAT to reveal underlying metabolic relationships. Numerous positive and negative correlations have been found between the differential metabolites in the serum, liver, muscle and eWAT (Supplementary table S16). In ND-fed ACE2 KO mice, more intra-tissue correlations were found in the serum. In HFD-fed ACE2 KO mice, both the serum and the muscle shared a similar number of intra-tissue metabolite correlations

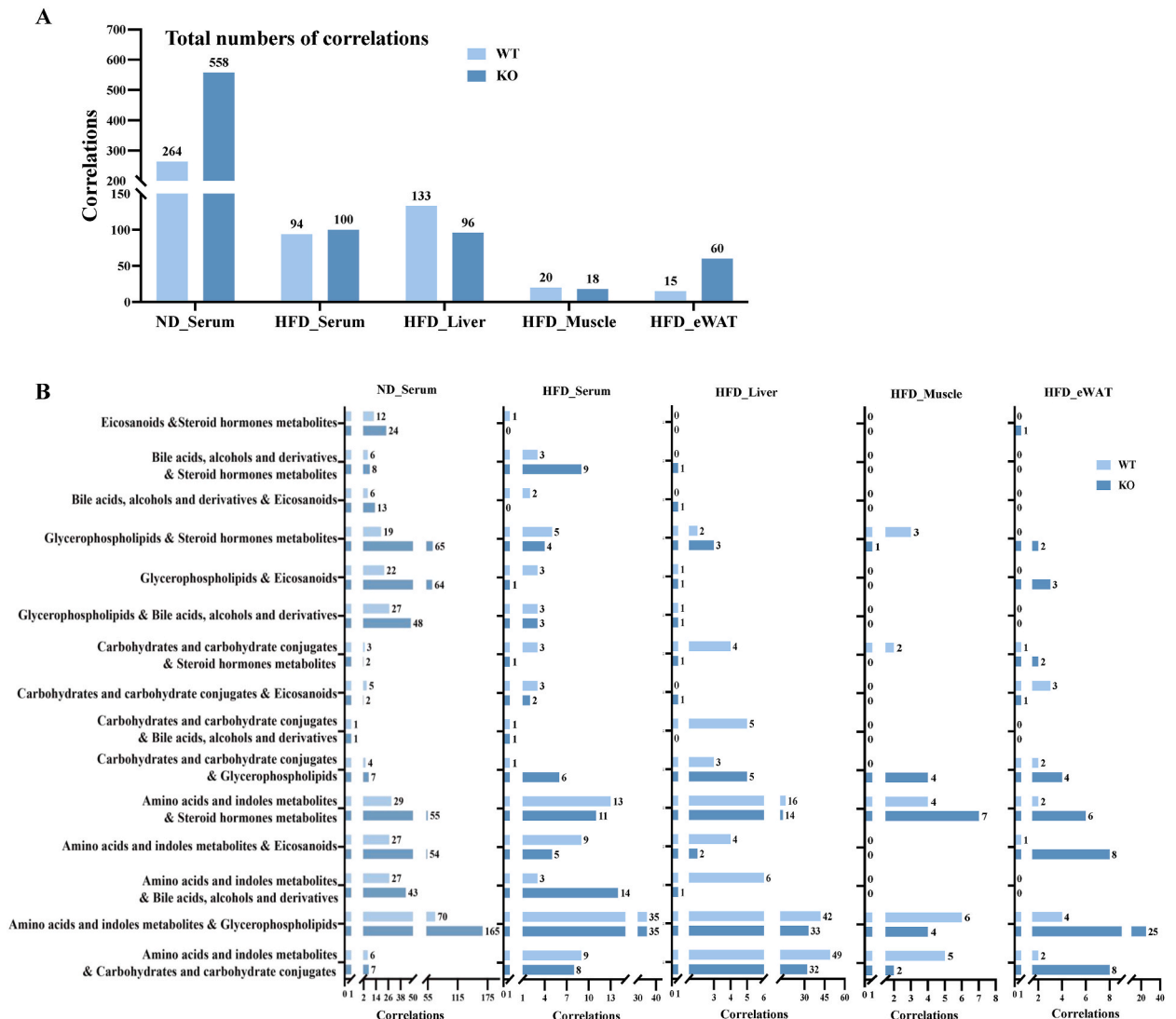


**Fig. 4.** Correlations in differential metabolites within tissues affected by ACE2 deletion. A. The bar chart displayed the total number of significantly different metabolite correlations within the six metabolite classes (amino acids and indoles metabolites; carbohydrates and carbohydrates conjugates; glycerophospholipids; bile acids, alcohols, and derivatives; eicosanoids; steroid hormones metabolites) in serum (ND\_Serum) of ND-fed ACE2 KO and WT mice, and in serum (HFD\_Serum), liver (HFD\_Liver), muscle (HFD\_Muscle) and eWAT (HFD\_eWAT) of HFD-fed ACE2 KO and WT mice. B. Comparative analysis of intra-tissue metabolite correlations in WT and ACE2 KO group. Fifteen kinds of remarkably different intra-tissue metabolite correlations (as showed in the Y-axis) were detected within the six metabolite classes (amino acids and indoles metabolites; carbohydrates and carbohydrates conjugates; glycerophospholipids; bile acids, alcohols, and derivatives; eicosanoids; steroid hormones metabolites) in WT and ACE2 KO group. The bar chart displayed the number of significantly different metabolite correlations for each of the 15 kinds of intra-tissue metabolite correlations in serum (ND\_Serum) of ND-fed ACE2 KO and WT mice, and in serum (HFD\_Serum), liver (HFD\_Liver), muscle (HFD\_Muscle) and eWAT (HFD\_eWAT) of HFD-fed ACE2 KO and WT mice.

compared with WT mice. However, the intra-tissue correlations were substantially reduced in liver while dramatically increased in eWAT (Fig. 4A, Supplementary table S16). Comparative analysis of intra-tissue metabolite correlations showed that amino acids and indoles metabolites had the strongest correlations with other metabolites in all the five pair-wise tissues, especially correlations between the amino acids and indoles metabolites with glycerophospholipids (Fig. 4B, Supplementary figs. S4A–E, Supplementary table S16). These differences in the correlations among the metabolites between the groups imply that metabolism is differentially organized due to the losing of ACE2 and reveal how networks within and among tissues are rewired by ACE2 deletion.

#### 4. Discussion

ACE2 knockout mice exhibit multiorgan energy metabolism disorders, but the underlying mechanisms and inter-tissue linkages are not fully understood. In the current study, we performed an untargeted metabolomics analysis in a collection of serum from ACE2 KO and WT mice fed on both ND and HFD, and three key metabolic tissues (liver, skeletal muscle and eWAT) after HFD treatment. To our knowledge, this is the first attempt to investigate the metabolomics profiling of ACE2 KO mice. We not only confirmed several previously reported findings, such as the decrease of serum Trp in ACE2 KO mice [25–27], but also expanded on them with many other altered metabolites in metabolite classes: carbohydrates and carbohydrates conjugates; glycerophospholipids; bile acids, alcohols, and derivatives; eicosanoids; and steroid hormones metabolites. Our study revealed significant differences in the response of different tissues to ACE2 deletion, but there is also a certain degree of correlation. These results confirmed the association between metabolism and ACE2, which were not only in line with our previous reports, but also provided new insights for exploring the mechanism of ACE2 regulating metabolism.

Prior studies have noted the importance of amino acid in human metabolism [38,39]. Valine, one of three branched-chain amino acids (BCAA), is recognized as a potential molecular marker for predicting type 2 diabetes [39]. A catabolic intermediate of valine, 3-hydroxyisobutyrate (3-HIB), is associated with the regulation of *trans*-endothelial fatty acid transport and lipid accumulation in muscles, contributing to insulin resistance [40,41]. The relationship between elevated blood BCAA levels and insulin resistance works in both directions [42]. Valine was upregulated in the serum of ACE2 KO ND mice, suggesting that ACE2 deletion might result in insulin resistance via increased valine.

PAGln and PAGly, produced by phenylacetic acid in the liver, are associated with an increased risks of cardiovascular disease through their interaction with adrenergic receptors [43]. The activation of the adrenergic system has been linked to alterations in glycolipid metabolism and insulin resistance [44]. Furthermore, elevated levels of PAGly serve as a potential biomarker for drug-induced phospholipidosis (PLD), a condition resulting from the inhibition of  $\beta$ -oxidation [45]. PLD is a lysosomal storage disorder characterized by the excessive accumulation of substances within tissues, leading to subsequent inflammation [46]. Our results showed that PAGly levels were upregulated in both ACE2 KO ND and HFD mice.

Given that the ACE2 protein facilitates the function of the amino acid transporter B(O)AT1 [26], our results indeed revealed that deficiency of ACE2 led to a reduction in neutral amino acids, including L-threonine and asparagine, as well as essential amino acids, such as DL-tryptophan and D-(+)-tryptophan. Besides, essential amino acid L-methionine was also decreased in ACE2 KO ND mice. A recent study demonstrated that serum tryptophan levels were not normalized after tryptophan supplementation in ACE2 KO mice, whereas an increase in tryptophan levels was observed in mice receiving adeno-associated virus-ACE2 [27]. Meanwhile, tryptophan is known to enable intestinal L-cells and  $\alpha$ -cells of the islets to promote GLP-1 secretion, and to protect mitochondrial function, thereby ameliorating oxidative stress in islet  $\beta$ -cells [27]. According to our results, DL-tryptophan was downregulated in serum of ACE2 KO ND mice, and in serum and muscle of ACE2 KO HFD mice, but was conversely upregulated in liver of ACE2 KO HFD mice, which need to be further investigated.

Some studies indicated that asparagine was higher in T2DM patients through upregulation of the mTORC1 pathway [47,48], while others have suggested that asparagine serves as a protective biomarker against diabetes risk [49]. In our study, L-asparagine was decreased in the serum of ACE2 KO ND mice, whereas asparagine increased in the serum of ACE2 KO HFD mice. Besides, both asparagine and L-asparagine were upregulated in the liver of ACE2 KO HFD mice. L-argininosuccinic acid was upregulated in the serum of ACE2 KO ND mice and argininosuccinic acid was increased in the muscle of ACE2 KO HFD mice in this study, which were involved in the urea cycle and should be further investigated. Previous study has shown that patients with T2DM exhibited higher levels of arginine and lower levels of ornithine, which also participates in the urea cycle [50]. However, another study demonstrated that serum ornithine levels were positively associated with diabetes risk [51]. Both DL-arginine and ornithine were elevated in liver and muscle of ACE2 KO HFD mice, a finding that requires further clarification. Our study indicated L-ergothioneine levels were lessened in liver, muscle, and eWAT of HFD ACE2 KO mice. L-ergothioneine is known to upregulate anti-oxidant cytoprotective genes, and downregulate NF- $\kappa$ B expression by activating Nrf2 so as to alleviate diabetes-induced renal dysfunction [52].

The cortex in the adrenal gland mainly secretes three classes of steroid hormone, including mineralcorticoid (aldosterone), glucocorticoid (cortisol) and androgens [53]. Elevated levels of aldosterone, cortisol, cortisone, and corticosterone are stimulated by adrenocorticotropic hormone (ACTH) and AngII [54]. Aldosterone regulates sodium resorption and fluid levels [55], and high levels of cortisol are associated with type 2 diabetes [56,57]. As expected, corticosterone levels were found to be high in ACE2 KO ND and HFD mice.

Glucose-6 phosphate (G6P) plays a key role in the metabolism of the liver, participating in glycolysis, glycogen synthesis, de novo lipogenesis, the pentose phosphate pathway, and the hexosamine pathway [58]. Xylulose-5-phosphate (X5P) is an intermediate of the pentose phosphate pathway, derived directly from two glycolytic intermediates, including glyceraldehyde-3-phosphate (GAP) and fructose-6-P (F6P) [59]. G6P and X5P can partially activate the carbohydrate response element binding protein (ChREBP), enhancing de novo lipogenesis [60]. The downregulation of serum G6P and X5P in ACE2 KO ND mice may suggest that hepatic impairment [21],

indicating that glucose cannot be efficiently converted into lipids, resulting in aggravated hyperglycemia environment, which should be further investigated. However, G6P, rather than X5P, is an essential modulator of ChREBP translocation and transcriptional activity in liver, inversely correlated with glucose 6-phosphate dehydrogenase (G6PDH) activity, the rate-limiting enzyme of the pentose phosphate pathway [61]. In ACE2 KO HFD mice, the decreased G6P in the liver reduced ChREBP activity and blunted the expression of related target genes in response to glucose. In addition, our results demonstrated that serum gluconic acid was elevated in ACE2 KO HFD mice. Previous studies have confirmed that increased plasma gluconic acid levels are observed in individuals with diabetes, particularly in those with diabetic retinopathy [62]. Notably, Indoxyl- $\beta$ -D-glucuronide was significantly upregulated in the serum of ACE2 KO HFD mice in our report. Indoxyl- $\beta$ -D-glucuronide, an indolic uremic toxins derived from tryptophan metabolism, had proinflammatory, procoagulant, prooxidant, and proapoptotic damages on the cardiovascular system [63].

Lipids serve three fundamental functions, including energy reservoir, components of biological membranes, and agents in signal transduction [64]. The dysregulation of lipid metabolism enhances the risk of prediabetes and type 2 diabetes [39]. As highlighted in the literature review, lipids are complexed because their biological functions are influenced by the chain length and saturation [65]. Phospholipids, major components of cellular membranes, play a critical role in hepatic lipid metabolism [39]. Phosphatidylcholine (PC) and phosphatidylethanolamine (PE) are the most and the second most abundant phospholipid, respectively, with PE capable of being converted into PC [65]. Interestingly, specific phospholipid species are associated with diabetes, rather than their total concentrations [65]. Notably, PC (14:0e/6:0) was found to be decreased in both serum and muscle. Despite these promising results, the question of whether individual PCs with varying chain lengths and saturation levels induce insulin resistance await further study.

Lysophosphatidylcholine (LPC) is identified as the main component of oxidatively damaged low-density lipoprotein (oxLDL) [66]. However, LPC acts as a double-edged sword [67]. Interestingly, LPC levels in serum are negatively correlated with type 2 diabetes [68]. In addition, LPC can inhibit inflammation to some extent [67]. In line with the present results, a previous study has demonstrated that LPC (22:1), LPC (20:1) and LPC (20:0) are negatively aligned with insulin resistance [69]. Therefore, whether LPC decreases blood glucose or exerts an anti-inflammatory effect remains to be elucidated.

12-hydroxyeicosatetraenoic acid (12-HETE), the primary product of 12-lipoxygenase (12-LOX), plays a crucial role in thrombogenesis, atherosclerosis, inflammation and oxidative stress, contributing to the development of diabetes and its associated complications [70,71]. Serum 12-HETE levels were indeed upregulated in ACE2 KO ND and HFD mice. Prostaglandins, activated by the ACE2/Ang(1–7)/Mas pathway, have been shown to mitigate diabetes-induced cardiovascular complications by reducing NADPH oxidase (NOX) activity [72]. Additionally, thromboxane-dependent platelet activation is implicated in atherothrombosis in T2DM [73, 74]. In our study, levels of prostaglandin E2 were found to be decreased in the serum and liver of ACE2 KO HFD mice. Meanwhile, levels of thromboxane B3 were increased in serum and epididymal white adipose tissue, while levels of thromboxane B1 were reduced in the liver of ACE2 KO HFD mice, which were worthy of further research and exploration.

Our results indicated that serum tryptophan were reduced both in ND-fed and HFD-fed ACE2 KO mice, and what's interesting is that serum Trp is also significantly decreased in COVID-19 patients [75]. After SARS-CoV-2 infection, loss of ACE2 results in high levels of AngII, then activates inflammatory signaling in the gastrointestinal tract [76]. Besides, downregulated intestinal ACE2-B(0)AT1 negatively impact neutral amino acids, especially tryptophan, then decreased tryptophan suppresses GLP-1 and GIP secretion and absorbs overwhelmed glucose [77]. Furthermore, reduced tryptophan causes few antimicrobial peptides release via inhibiting mTOR pathway, thereby generating gut microbiota dysbiosis [26]. As high fat diet itself can cause dysbiosis of intestinal microflora, ACE2 deficiency may worsen this situation.

Despite unveiling novel insights into metabolite changes across several tissues in ACE2 KO mice subjected to different diets, this study encompasses certain limitations. In this study, metabolites in the liver, skeletal muscle, and eWAT of ND-fed ACE2 KO and WT mice were not analyzed, hence the exploration of diet-dependent responses to ACE2 deletion was confined to serum analysis. Additionally, the study lacked biological experimental validation of the metabolite. However, some findings were corroborated by existing literature, which may partly mitigate this limitation. Moreover, our study was conducted using a mouse model with ACE2 deletion, so that the results in human beings with ACE2 polymorphisms might differ.

## 5. Conclusion

In conclusion, this study provides a comprehensive dataset of metabolites across a wide collection of tissues under varying dietary conditions, and our analysis provides a detailed landscape of differential metabolites resulting from ACE2 deletion across these tissues. These insights contribute new knowledge on the biological processes underlying impaired energy metabolism in ACE2 KO mice and provide potential clues towards understanding the mechanism underling the metabolic disorders in human beings associated with the ACE2 polymorphisms.

### Funding statement

This work was supported by grants from National Natural Science Foundation of China (82270897, 82000825, 82070850); Beijing Natural Science Foundation (7232231); Beijing Hospitals Authority Youth Programme (QML20230207).

### Data availability statement

Data will be made available on request.

## CRediT authorship contribution statement

**Lili Zhao:** Writing – original draft, Investigation, Formal analysis, Data curation. **Weili Yang:** Writing – review & editing, Writing – original draft, Investigation, Funding acquisition, Formal analysis, Data curation. **Wenyi Ji:** Investigation, Data curation. **Qiuyue Pan:** Investigation, Formal analysis. **Jinkui Yang:** Resources. **Xi Cao:** Writing – review & editing, Resources, Methodology, Funding acquisition, Formal analysis, Data curation.

## Declaration of competing interest

The authors declare that they have no known competing financial interests or personal relationships that could have appeared to influence the work reported in this paper.

## Appendix ASupplementary data

Supplementary data to this article can be found online at <https://doi.org/10.1016/j.heliyon.2024.e27472>.

## References

- [1] R. Pazoki, A. Dehghan, E. Evangelou, et al., Genetic Predisposition to high blood Pressure and lifestyle factors: Associations with midlife blood pressure levels and cardiovascular events, *Circulation* 137 (2018) 653–661.
- [2] A. Jan, M. Saeed, R.A. Mothana, et al., Association of CYP2C9\*2 allele with sulphonylurea-induced hypoglycaemia in type 2 diabetes mellitus patients: a pharmacogenetic study in Pakistani pashtun population, *Biomedicines* 11 (2023).
- [3] T.-T. Shi, F.-Y. Yang, C. Liu, et al., Angiotensin-converting enzyme 2 regulates mitochondrial function in pancreatic  $\beta$ -cells, *Biochem. Biophys. Res. Commun.* 495 (2018) 860–866.
- [4] F. Zhang, C. Liu, L. Wang, et al., Antioxidant effect of angiotensin (1-7) in the protection of pancreatic  $\beta$  cell function, *Mol. Med. Rep.* 14 (2016) 1963–1969.
- [5] X. Cao, L.N. Song, Y.C. Zhang, et al., Angiotensin-converting enzyme 2 inhibits endoplasmic reticulum stress-associated pathway to preserve nonalcoholic fatty liver disease, *Diabetes Metabol. Res. Rev.* 35 (2019).
- [6] X. Cao, F.-Y. Yang, Z. Xin, et al., The ACE2/Ang-(1-7)/Mas axis can inhibit hepatic insulin resistance, *Mol. Cell. Endocrinol.* 393 (2014) 30–38.
- [7] C. Liu, X.H. Lv, H.X. Li, et al., Angiotensin-(1-7) suppresses oxidative stress and improves glucose uptake via Mas receptor in adipocytes, *Acta Diabetol.* 49 (2012) 291–299.
- [8] L.N. Song, J.Y. Liu, T.T. Shi, et al., Angiotensin-(1-7), the product of ACE2 ameliorates NAFLD by acting through its receptor Mas to regulate hepatic mitochondrial function and glycolipid metabolism, *Faseb. J.* 34 (2020) 16291–16306.
- [9] X. Cao, T.T. Shi, C.H. Zhang, et al., ACE2 pathway regulates thermogenesis and energy metabolism, *Elife* 11 (2022).
- [10] X. Cao, X.M. Lu, X. Tuo, et al., Angiotensin-converting enzyme 2 regulates endoplasmic reticulum stress and mitochondrial function to preserve skeletal muscle lipid metabolism, *Lipids Health Dis.* 18 (2019) 207.
- [11] X. Cao, F. Yang, T. Shi, et al., Angiotensin-converting enzyme 2/angiotensin-(1-7)/Mas axis activates Akt signaling to ameliorate hepatic steatosis, *Sci. Rep.* 6 (2016) 21592.
- [12] Y. Cao, L. Li, Z. Feng, et al., Comparative genetic analysis of the novel coronavirus (2019-nCoV/SARS-CoV-2) receptor ACE2 in different populations, *Cell Discov.* 6 (2020) 11.
- [13] J. Lumpuy-Castillo, C. Vales-Villamarín, I. Mahfíllo-Fernández, et al., Association of ACE2 polymorphisms and derived haplotypes with obesity and hyperlipidemia in female Spanish adolescents, *Front Cardiovasc Med* 9 (2022) 888830.
- [14] A. Yousif, R. Mir, J. Javid, et al., Clinical utility of amplification refractory mutation system-based PCR and mutation-specific PCR for precise and rapid genotyping of angiotensin-converting enzyme 1 (ACE1-rs4646996 D>I) and angiotensin-converting enzyme 2 (ACE2-rs4240157T>C) gene variations in coronary artery disease and their strong association with its disease susceptibility and progression, *Diagnostics* 12 (2022).
- [15] G. Huang, Q. Liang, Y. Wang, et al., Association of ACE2 gene functional variants with gestational diabetes mellitus risk in a southern Chinese population, *Front. Endocrinol.* 13 (2022) 1052906.
- [16] C. Liu, Y. Li, T. Guan, et al., ACE2 polymorphisms associated with cardiovascular risk in Uygurs with type 2 diabetes mellitus, *Cardiovasc. Diabetol.* 17 (2018) 127.
- [17] Y. Pan, T. Wang, Y. Li, et al., Association of ACE2 polymorphisms with susceptibility to essential hypertension and dyslipidemia in Xinjiang, China, *Lipids Health Dis.* 17 (2018) 241.
- [18] C. Liu, J. Pei, Y. Lai, et al., Association of ACE2 variant rs4646188 with the risks of atrial fibrillation and cardioembolic stroke in Uygur patients with type 2 diabetes, *BMC Cardiovasc. Disord.* 21 (2021) 103.
- [19] M.J. Niu, J.K. Yang, S.S. Lin, et al., Loss of angiotensin-converting enzyme 2 leads to impaired glucose homeostasis in mice, *Endocrine* 34 (2008) 56–61.
- [20] X. Cao, L.-N. Song, J.-K. Yang, ACE2 and energy metabolism: the connection between COVID-19 and chronic metabolic disorders, *Clinical Science* 135 (2021) 535–554.
- [21] T.S. Di Wu, Xiaobo Yang, Jian-Xin Song, Mingliang Zhang, Chengye Yao, Liu Wen, Muhan Huang, Yu Yuan, Qingyu Yang, Tingju Zhu, Jiqian Xu, Jingfang Mu, Yaxin Wang, Hong Wang, Tang Tang, Yujie Ren, Yongran Wu, Shu-Hai Lin, Yang Qiu, Ding-Yu Zhang, You Shang, Xi Zhou, Plasma metabolomic and lipidomic alterations associated with COVID-19, *Natl. Sci. Rev.* 7 (7) (2020) 1157–1168.
- [22] M. Ciccarelli, F. Merciai, A. Carrizzo, et al., Untargeted lipidomics reveals specific lipid profiles in COVID-19 patients with different severity from Campania region (Italy), *J. Pharm. Biomed. Anal.* 217 (2022) 114827.
- [23] M.A. Elrayess, F.S. Cyprian, A.M. Abdallah, et al., Metabolic signatures of type 2 diabetes mellitus and hypertension in COVID-19 patients with different disease severity, *Front. Med.* 8 (2021) 788687.
- [24] B. Bakhshandeh, S.G. Sorboni, A.R. Javanmard, et al., Variants in ACE2; potential influences on virus infection and COVID-19 severity, *Infect. Genet. Evol.* 90 (2021) 104773.
- [25] D. Singer, S.M. Camargo, T. Ramadan, et al., Defective intestinal amino acid absorption in Ace2 null mice, *Am. J. Physiol. Gastrointest. Liver Physiol.* 303 (2012) G686–G695.
- [26] T. Hashimoto, T. Perlot, A. Rehman, et al., ACE2 links amino acid malnutrition to microbial ecology and intestinal inflammation, *Nature* 487 (2012) 477–481.
- [27] Q. Chen, F. Gao, Y. Gao, et al., Intestinal ACE2 regulates glucose metabolism in diet-induced obese mice through a novel gut-islet axis mediated by tryptophan, *Obesity* 31 (2023) 1311–1325.
- [28] W. Yang, Z. Xia, Y. Zhu, et al., Comprehensive study of untargeted metabolomics and 16S rRNA reveals the mechanism of fecal microbiota transplantation in improving a mouse model of T2D, *Diabetes Metab Syndr Obes* 16 (2023) 1367–1381.

- [29] M. Alemany, Estrogens and the regulation of glucose metabolism, *World J. Diabetes* 12 (2021) 1622–1654.
- [30] Y. Meng, L.L. Thornburg, K.M. Hoeger, et al., Association between sex steroid hormones and subsequent hyperglycemia during pregnancy, *Front. Endocrinol.* 14 (2023) 1213402.
- [31] M. Shahwan, F. Alhumaydhi, G.M. Ashraf, et al., Role of polyphenols in combating Type 2 Diabetes and insulin resistance, *Int. J. Biol. Macromol.* 206 (2022) 567–579.
- [32] Y. Liu, L. Gan, B. Zhao, et al., Untargeted metabolomic profiling identifies serum metabolites associated with type 2 diabetes in a cross-sectional study of the Alpha-Tocopherol, Beta-Carotene Cancer Prevention (ATBC) Study, *Am. J. Physiol. Endocrinol. Metab.* 324 (2023) E167–e175.
- [33] B. Arneith, R. Arneith, M. Shams, *Metabolomics of type 1 and type 2 diabetes*, *Int. J. Mol. Sci.* 20 (2019).
- [34] L. Yan, P. Han, J. Man, et al., Discovery of lipid profiles of type 2 diabetes associated with hyperlipidemia using untargeted UPLC Q-TOF/MS-based lipidomics approach, *Clin. Chim. Acta* 520 (2021) 53–62.
- [35] A.J. Xie, C.T. Mai, Y.Z. Zhu, et al., Bile acids as regulatory molecules and potential targets in metabolic diseases, *Life Sci.* 287 (2021) 120152.
- [36] P. Luo, M.H. Wang, Eicosanoids,  $\beta$ -cell function, and diabetes, *Prostag. Other Lipid Mediat.* 95 (2011) 1–10.
- [37] K. Tuomisto, J. Palmu, T. Long, et al., A plasma metabolite score of three eicosanoids predicts incident type 2 diabetes: a prospective study in three independent cohorts, *BMJ Open Diabetes Res Care* 10 (2022).
- [38] M.D. Neinast, C. Jang, S. Hui, et al., Quantitative analysis of the whole-body metabolic fate of branched-chain amino acids, *Cell Metab* 29 (2019) 417–429 e414.
- [39] M. Guasch-Ferre, A. Hruby, E. Toledo, et al., Metabolomics in prediabetes and diabetes: a systematic review and meta-analysis, *Diabetes Care* 39 (2016) 833–846.
- [40] C. Jang, S.F. Oh, S. Wada, et al., A branched-chain amino acid metabolite drives vascular fatty acid transport and causes insulin resistance, *Nat Med* 22 (2016) 421–426.
- [41] C. Nie, T. He, W. Zhang, et al., Branched chain amino acids: beyond nutrition metabolism, *Int. J. Mol. Sci.* 19 (2018).
- [42] D.G. Le Couteur, S.M. Solon-Biet, V.C. Cogger, et al., Branched chain amino acids, aging and age-related health, *Ageing Res. Rev.* 64 (2020) 101198.
- [43] I. Nemet, P.P. Saha, N. Gupta, et al., A cardiovascular disease-linked gut microbial metabolite acts via adrenergic receptors, *Cell* 180 (2020) 862–877 e822.
- [44] M. Ciccarelli, G. Santulli, V. Pascale, et al., Adrenergic receptors and metabolism: role in development of cardiovascular disease, *Front. Physiol.* 4 (2013) 265.
- [45] H. Kamiguchi, M. Murabayashi, I. Mori, et al., Biomarker discovery for drug-induced phospholipidosis: phenylacetyl-glycine to hippuric acid ratio in urine and plasma as potential markers, *Biomarkers* 22 (2017) 178–188.
- [46] H. Kamiguchi, M. Yamaguchi, M. Murabayashi, et al., Method development and validation for simultaneous quantitation of endogenous hippuric acid and phenylacetyl-glycine in rat urine using liquid chromatography coupled with electrospray ionization tandem mass spectrometry, *J. Chromatogr., B: Anal. Technol. Biomed. Life Sci.* 1035 (2016) 76–83.
- [47] H. Zhu, M. Bai, X. Xie, et al., Impaired amino acid metabolism and its correlation with diabetic kidney disease progression in type 2 diabetes mellitus, *Nutrients* 14 (2022).
- [48] A.S. Krall, S. Xu, T.G. Graeber, et al., Asparagine promotes cancer cell proliferation through use as an amino acid exchange factor, *Nat. Commun.* 7 (2016) 11457.
- [49] C.M. Rebolz, B. Yu, Z. Zheng, et al., Serum metabolomic profile of incident diabetes, *Diabetologia* 61 (2018) 1046–1054.
- [50] Y.F. Cao, J. Li, Z. Zhang, et al., Plasma levels of amino acids related to urea cycle and risk of type 2 diabetes mellitus in Chinese adults, *Front. Endocrinol.* 10 (2019) 50.
- [51] S.H. Gunther, C.M. Khoo, E.S. Tai, et al., Serum acylcarnitines and amino acids and risk of type 2 diabetes in a multiethnic Asian population, *BMJ Open Diabetes Res Care* 8 (2020).
- [52] A. Dare, M.L. Channa, A. Nadar, L-ergothioneine and its combination with metformin attenuates renal dysfunction in type-2 diabetic rat model by activating Nrf2 antioxidant pathway, *Biomed. Pharmacother.* 141 (2021) 111921.
- [53] B.D. Freedman, P.B. Kempna, D.L. Carlone, et al., Adrenocortical zonation results from lineage conversion of differentiated zona glomerulosa cells, *Dev. Cell* 26 (2013) 666–673.
- [54] K. Wellman, R. Fu, A. Baldwin, et al., Transcriptomic response dynamics of human primary and immortalized adrenocortical cells to steroidogenic stimuli, *Cells* 10 (2021).
- [55] J.M. Connell, S.M. MacKenzie, E.M. Freel, et al., A lifetime of aldosterone excess: long-term consequences of altered regulation of aldosterone production for cardiovascular function, *Endocr. Rev.* 29 (2008) 133–154.
- [56] S. Patel, A. Rauf, H. Khan, et al., Renin-angiotensin-aldosterone (RAAS): the ubiquitous system for homeostasis and pathologies, *Biomed. Pharmacother.* 94 (2017) 317–325.
- [57] B.M. Patel, A.A. Mehta, Aldosterone and angiotensin: role in diabetes and cardiovascular diseases, *Eur. J. Pharmacol.* 697 (2012) 1–12.
- [58] F. Rajas, A. Gautier-Stein, G. Mithieux, Glucose-6 phosphate, A central hub for liver carbohydrate metabolism, *Metabolites* 9 (2019).
- [59] T. Kabashima, T. Kawaguchi, B.E. Wadzinski, et al., Xylulose 5-phosphate mediates glucose-induced lipogenesis by xylulose 5-phosphate-activated protein phosphatase in rat liver, *Proc. Natl. Acad. Sci. U. S. A.* 100 (2003) 5107–5112.
- [60] K. Iizuka, W. Wu, Y. Horikawa, J. Takeda, Role of glucose-6-phosphate and xylulose-5-phosphate in the regulation of glucose-stimulated gene expression in the pancreatic  $\beta$  cell line, *INS-1E*, *Endocr. Rev.* 60 (2013) 473–482.
- [61] R. Dentin, L. Tomas-Cobos, F. Fougelle, et al., Glucose 6-phosphate, rather than xylulose 5-phosphate, is required for the activation of ChREBP in response to glucose in the liver, *J. Hepatol.* 56 (2012) 199–209.
- [62] L. Chen, C.Y. Cheng, H. Choi, et al., Plasma metabolomic profiling of diabetic retinopathy, *Diabetes* 65 (2016) 1099–1108.
- [63] M. Sallee, L. Dou, C. Cerini, et al., The aryl hydrocarbon receptor-activating effect of uremic toxins from tryptophan metabolism: a new concept to understand cardiovascular complications of chronic kidney disease, *Toxins* 6 (2014) 934–949.
- [64] T.A. Lydic, Y.H. Goo, Lipidomics unveils the complexity of the lipidome in metabolic diseases, *Clin. Transl. Med.* 7 (2018) 4.
- [65] Q. Yang, A. Vijayakumar, B.B. Kahn, Metabolites as regulators of insulin sensitivity and metabolism, *Nat. Rev. Mol. Cell Biol.* 19 (2018) 654–672.
- [66] Z. Zhou, P. Subramanian, G. Sevilimis, et al., Lipoprotein-derived lysophosphatidic acid promotes atherosclerosis by releasing CXCL1 from the endothelium, *Cell Metab* 13 (2011) 592–600.
- [67] P. Liu, W. Zhu, C. Chen, et al., The mechanisms of lysophosphatidylcholine in the development of diseases, *Life Sci.* 247 (2020) 117443.
- [68] S.H. Law, M.L. Chan, G.K. Marathe, et al., An updated review of lysophosphatidylcholine metabolism in human diseases, *Int. J. Mol. Sci.* 20 (2019).
- [69] K.T. Tonks, A.C. Coster, M.J. Christopher, et al., Skeletal muscle and plasma lipidomic signatures of insulin resistance and overweight/obesity in humans, *Obesity* 24 (2016) 908–916.
- [70] S. Chen, H. Zou, Key role of 12-lipoxygenase and its metabolite 12-hydroxyeicosatetraenoic acid (12-HETE) in diabetic retinopathy, *Curr. Eye Res.* 47 (2022) 329–335.
- [71] A.D. Dobrian, M.A. Morris, D.A. Taylor-Fishwick, et al., Role of the 12-lipoxygenase pathway in diabetes pathogenesis and complications, *Pharmacol. Ther.* 195 (2019) 100–110.
- [72] M.H. Yousif, G.S. Dhaunsi, B.M. Makki, et al., Characterization of Angiotensin-(1-7) effects on the cardiovascular system in an experimental model of type-1 diabetes, *Pharmacol. Res.* 66 (2012) 269–275.
- [73] F. Santilli, P. Simeone, R. Liani, et al., Platelets and diabetes mellitus, *Prostag. Other Lipid Mediat.* 120 (2015) 28–39.
- [74] C. Patrono, B. Rocca, Less thromboxane, longer life, *J. Am. Coll. Cardiol.* 80 (2022) 251–255.

- [75] W.H. Qin, C.L. Liu, Y.H. Jiang, et al., Gut ACE2 expression, tryptophan deficiency, and inflammatory responses the potential connection that should not Be ignored during SARS-CoV-2 infection, *Cell Mol Gastroenterol Hepatol* 12 (2021) e1514, 1514-1516.
- [76] S.D. Viana, S. Nunes, F. Reis, ACE2 imbalance as a key player for the poor outcomes in COVID-19 patients with age-related comorbidities - role of gut microbiota dysbiosis, *Ageing Res. Rev.* 62 (2020) 101123.
- [77] J.M. Penninger, M.B. Grant, J.J.Y. Sung, The role of angiotensin converting enzyme 2 in modulating gut microbiota, intestinal inflammation, and coronavirus infection, *Gastroenterology* 160 (2021) 39–46.